# Research on Variable Step Adaptive Speed Controller for Marine Diesel Engine Based on Active Disturbance Rejection Control Algorithm

Shu Haoyu, Li Xuemin

*Abstract*— **This manuscript conducts research on the speed control of large-power high-speed diesel engines for marine. In view of the poor performance for nonlinear system and weak reject disturbance ability of the traditional PID controller , this manuscript designs a new type of speed controller based on crankshaft angle. The new speed controller is designed based on the active disturbance rejection control algorithm (ADRC), and the parameters of the ADRC are optimized by the beetle antennae search algorithm (BAS) in real time. Subsequently, a BAS with variable search step size (VABAS) and PID with variable parameters (VP-PID) were designed. In VABAS, the antennae length of beetle antennae varies with the change of reference speed. The simulation experiment were conducted on cylinder-by-cylinder mean value engine model (MVEM), the results demonstrate that compared with VP-PID controllers, VABAS-ADRC has better control effects in dealing with nonlinear behavior and disturbances of marine diesel engines. Finally, in order to reduce the computational complexity of the algorithm and increase the optimization efficiency of VABAS, the three parameters to be optimized in ADRC were reduced to one based on experience, and simulation experiments were conducted, the results demonstrate that single parameter VABAS-ADRC (SP-VABAS-ADRC) has similar control performance to simultaneously optimizing three parameters.**

## I. INTRODUCTION

The speed control of diesel engines inherently possesses strong nonlinear characteristics. When a marine is operating at sea, the water surface environment is complex, and the waves can cause severe disturbances to the speed of the marine diesel engine through propellers, which can also make it difficult to control the speed of the marine diesel engine.

Most of the speed control devices used in the current shipbuilding industry use PID algorithm. The PID control algorithm, as a typical linear control algorithm, has the advantages of simple design and low computational complexity. However, when facing systems with strong nonlinearity and disturbances, the control effect is not satisfactory. The application cases in engineering often use segmented PID control, which means using different PID control parameters at different operating points. Although segmented PID can improve control performance to a certain extent, the parameters to be calibrated will also increase exponentially with the number of segments, making the calibration process more complex.

Shu Haoyu is with the College of Power and Energy Engineering, Harbin Engineering University, Harbin 150000 China (e-mail: shyheb123@163.com).

Li Xuemin is with the College of Power and Energy Engineering, Harbin Engineering University, Harbin 150000 China (e-mail: lxm@hrbeu.edu.cn).

With the continuous advancement of modern control theory, many new control algorithms have been proposed. These control algorithms have both advantages and disadvantages, and how to choose them in engineering applications should also be determined based on the characteristics of the controlled object. The sliding mode control algorithm (SMC) was born in the 1950s[1]. Subsequently, Soviet engineer V I. Utkin promotion has been widely applied in practical industry[2]. Its main application areas include motor control, aerospace, automotive control and so on[3-6]. The SMC has good robustness and can achieve finite time convergence through the design of the control law. However, due to the fast switching characteristics of sliding mode control algorithms near the sliding surface, chattering problems may arise during the control process. The model predictive control algorithm (MPC) was born in the 1960s[7]. It combines optimization ideas with control and is a typical representative in the field of optimization control, often applied in the chemical industry[8][9]. However, MPC is also a typical model-based control technique, and when the internal parameters of the model change, the control performance will deteriorate significantly. Meanwhile, the suppression effect of MPC on disturbances is also unsatisfactory. In existing research, when the controlled object has significant disturbances, disturbance observers are often used in combination[10-12]. The active disturbance rejection control algorithm (ADRC) was proposed by Han Jingqing in 1998[13][14]. It is an advanced control algorithm that integrates tracking path planning, disturbance rejection, and decoupling ideas. Another major advantage of ADRC is that it does not rely on model parameters. It has been proven in numerous studies and industrial practices that ADRC has excellent tracking performance and strong disturbance rejection capability. In the field of diesel engine control, there are also many scholars engaged in research on ADRC. The reference [15] used ADRC to design a new low-speed diesel engine speed controller. And a finite time convergent SMC control law was designed to improve the traditional extended state observer (ESO) for better control performance. The reference [16] applies ADRC to the speed control of marine diesel engines. Linear ADRC (LADRC) and nonlinear ADRC (NLADRC) controllers are designed separately, and switching strategies for the two controllers are developed based on the speed control characteristics of diesel engines. Simulation experiments have shown that the newly designed controller has better control performance compared to traditional controllers and single form ADRC controllers. The reference [17] conducted research on the application of ADRC in rail

pressure control of high-pressure common rail diesel engines. The designed sliding mode control law is introduced into the ADRC nonlinear error feedback link, combined with the feedforward control, to improve the control performance of diesel engine rail pressure under steady-state and dynamic conditions.

Although ADRC has excellent tracking performance and strong reject disturbance ability, there are many parameters to be calibrated. And diesel engine speed control has strong nonlinearity, even if ADRC is used to design the controller, it cannot achieve a set of parameters that can adapt to all diesel engine operating conditions. This undoubtedly poses a huge obstacle to the calibration process of the speed controller. In recent years, with the continuous upgrading of the computing power of microcontrollers, optimization algorithms such as swarm intelligence, neural networks, and reinforcement learning have been combined with PID to achieve real-time optimization of PID parameters. After comprehensive consideration of optimization efficiency and algorithm computation, this manuscript decides to choose BAS to optimize the control parameters of ADRC algorithm in real-time online, and adjust the length of antennae according to the current target speed of diesel engine, in order to achieve excellent performance of diesel engine speed control in the entire operating range.

In this manuscript, firstly, the cylinder-by-cylinder MVEM for 16-cylinder high power marine diesel engine is designed based on the design approach in the reference [10]. Then, considering that the ADRC controller has better control performance than PID, and the current microcontroller main frequency has been substantially increased than in the past, but PID is still used for diesel engine speed control in the project. So this manuscript decides to design a new speed controller based on ADRC.

However, ADRC has many parameters, the calibration process is cumbersome, and considering the nonlinear characteristics of diesel engine, it is difficult to realize excellent control performance under full operating conditions by a set of parameters. So this manuscript introduces the intelligent search algorithm BAS to adjust the parameters of ADRC online. Subsequently, VABAS-ADRC is proposed to avoid chattering at high control frequency. The excellent performance of the designed controller is demonstrated through simulation experiments. Finally, the three parameters to be optimized are reduced to one, and the SP-VABAS-ADRC is proposed, and the experiment proves that the new controller reduces the computational amount while, to some extent, maintaining the original control performance.

## II. PHYSICAL MODEL

In previous research on diesel engine control technology, the MVEM was mostly used for simulation verification. Moreover, the MVEM does not take into account the pressure changes of the cylinder within one cycle, so it cannot reflect

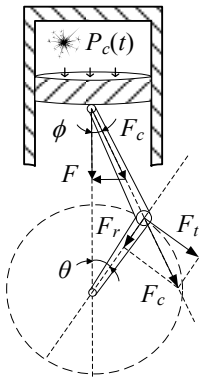


Figure 1. Figure 1. Force diagram of crank-link mechanism

the steady-state fluctuation phenomenon of diesel engine speed. This manuscript uses the modeling method from the reference [10] to build a cylinder-by-cylinder MVEM for a 16 cylinder high-power marine diesel engine. The force diagram of each cylinder and its corresponding crank train is shown in Fig. 1.

The acceleration of a diesel engine can be expressed by the following equation:

$$\dot{n}_e = \frac{30(M_{ip} - M_f - M_{load})}{\pi(J_e + J_l)} \tag{1}$$

where $n_e$ represents the diesel engine speed, $M_{ip}$ , $M_f$ , $M_{load}$ represents the difference between the indicated torque and the pumping torque, the frictional torque and the load torque respectively. $J_e$ and $J_l$ represents the equivalent inertia of the moving parts and inertia of the propeller and the spindle system respectively.

Both friction torque and load torque can be represented by the quadratic expression of diesel engine speed, so $M_{ip}$ is the key variable for modeling. By analyzing the force relationship in Fig. 1, $M_{ip}$ can be represented as:

$$M_{ip}(t) = \sum_{j=1}^{6} \frac{\pi \sin(\phi_j + \theta_j)}{4\cos\phi_j} r d^2 p_{c,j}(t) \tag{2}$$

where $r$ represents the radius of the crankshaft, $d$ represents the diameter of the cylinder.

After analysis, it can be concluded that if $p_c$ can be represented by a formula, the speed of the diesel engine can be modeled.

Based on the variation of a diesel engine working cycle, the working cycle is divided into 5 stages to model $p_c$ .

When the intake valve is opened and the exhaust valve is closed, it is considered that the cylinder pressure at this time is equal to the pressure inside the intake manifold:

$$p_{im} = p_0 + \int_0^t \frac{R_i T_{im}(t)(W_c(t) - W_{ic}(t))}{V_{im}} dt \tag{3}$$

where $R$ , $T$ and $V$ represents the gas constant, the temperature and the volume of the gas respectively. $W_c$ and $W_{ic}$ represents the mass flow rate of the compressor and the mass flow rate of the gas entering the cylinder respectively.

Similar to the previous content, when the exhaust valve is opened and the intake valve is closed, the cylinder pressure is considered to be equal to the pressure inside the exhaust manifold.

During the scavenging process, both the intake and exhaust valves open simultaneously. The pressure at the intake is equal to the scavenging pressure, and the pressure at the exhaust is equal to the ambient pressure. The pressure inside the cylinder can be obtained by cosine interpolation of the pressure from the intake to the exhaust.

The compression process can be regarded as a polytropic process, so the pressure and temperature of the process can be expressed as:

$$p_c(t) = p_{ivc}\left(\frac{V_{ivc}}{V(t)}\right)^{k_c} \tag{4}$$

$$T_c(t) = T_{ivc}\left(\frac{V_{ivc}}{V(t)}\right)^{k_c-1} \tag{5}$$

where $p_{ivc}$ , $V_{ivc}$ and $T_{ivc}$ represent respectively initial cylinder pressure, initial cylinder working volume, and initial temperature at this stage, $V$ represents real-time cylinder working volume, $k_c$ represents polytropic index.

The stage from the beginning of combustion to the opening of the exhaust valve can be regarded as composed of multiple constant volume combustion processes:

$$p_c(t)\dot{V}(t) = m_f q_L \eta_t \dot{x}(t) - m_{tot} c_v \dot{T}_c(t) \tag{6}$$

where $q_L$ represents the net heating value of the fuel, $\eta_t$ represents the proportion of the actual converted heat of the fuel combustion in the heat generated by the complete combustion of the fuel, $x$ represents the proportion of fuel that has been combusted, $m_{tot}$ represents the total mass of the actuating medium in the cylinder.

In (6), the fuel conversion efficiency $\eta_t$ can be expressed by the engine speed and air-fuel ratio:

$$\eta_t = (k_{t1}n_e^2 + k_{t2}n_e + k_{t3})(1 - k_{t4}\lambda^{k_{t5}}) \tag{7}$$

The $x$ can be represented by a combustion model. Considering the accuracy and computational complexity of the control model, a simple Weber combustion model is chosen:

$$x(t) = 1 - e^{-a\left(\frac{\varphi(t)-\varphi_{soc}}{\varphi_{doc}}\right)^{m+1}} \tag{8}$$

Finally, combined with the ideal gas state equation the cylinder pressure in the fifth section can be obtained.

$$p_c(t)V(t) = m_{tot}RT_c(t) \tag{9}$$

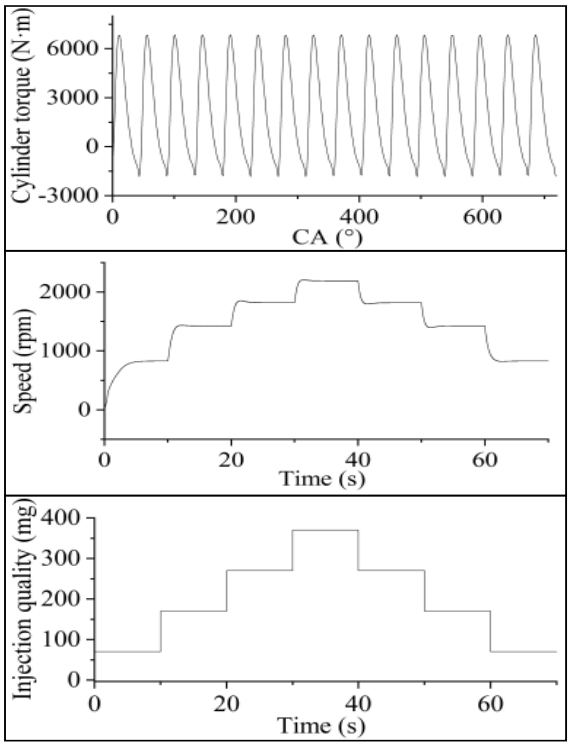


Figure 2. The open-loop operation results of cylinder-by-cylinder MVEM

The variation of cylinder torque with crankshaft angle are shown and the speed response of the diesel engine model at the open-loop fuel injection quantity shown in Fig. 2.

## III. CONTROLLER DESIGN

The adjustment of diesel engine fuel injection quantity is discrete. Under the premise of a fixed fuel injection advance angle, the crankshaft angle change corresponding to the interval between two fuel injections is fixed. In practical engineering applications, external interrupt triggering is generally used to perform fuel injection quantity calculations. So before designing the controller, it needs to be emphasized that the designed controller is a variable step controller, and its calculation step is related to the diesel engine speed, which is expressed as follows:

$$h(k) = \frac{30num_{stk}}{n_e(k)num_{cycl}} \tag{10}$$

where $num_{stk}$ represents the number of strokes in the diesel engine, and $num_{cycl}$ represents the number of cylinders in the diesel engine.

The first-order ADRC consists of a tracking differentiator (TD), nonlinear error feedback (NEF), and an extended state observer (ESO). The main idea is to consider the unmodeled internal dynamics and external disturbances of the controlled object as components of the total disturbance. Then, the total disturbance is observed and compensated for by ESO.

Taking into account both control performance requirements and computational complexity, the ADRC used in this manuscript is linear ADRC, which linearizes NEF and ESO.

TD is designed based on SMC theory and has the function of filtering out noise. The specific formula is as follows:

$$\begin{cases} v_1(k+1)=v_1(k)+h(k)v_2(k) \\ v_2(k+1)=v_2(k)+h(k)fst(v_1(k)-v(k),v_2(k),r,h_0(k)) \\ d=r_0h_0 \\ d_0=h_0d \\ m=v_1+h_0v_2 \\ a_0=\sqrt{d^2+8r_0|m|} \\ a=\begin{cases} v_2+\dfrac{a_0-d}{2}, & |m|>d_0 \\ v_2+\dfrac{y}{h_0}, & |m|\le d_0 \end{cases} \\ fst(v_1,v_2,r_0,h_0)=-\begin{cases} r_0 sign(a), & |a|>d \\ r_0\dfrac{a}{d}, & |a|\le d \end{cases} \end{cases} \tag{11}$$

In (11), $r_0$ and $h_0$ are the parameters to be adjusted. The value of $r_0$ determines the tracking speed of TD on the reference value, which is called the 'speed factor'. The $h_0$ has the function of filtering out noise and is called the 'filtering factor'. The $h_0$ is often a multiple of the program running step size. In a diesel engine speed controller, the program running step size is the time interval between two fuel injections at the current speed.

The manuscript uses a linear ESO without model information. Diesel engine speed control is a typical first-order system control problem. According to the internal model principle, ESO can be expressed as follows:

$$\begin{cases} \varepsilon(k)=z_1(k)-y(k) \\ z_1(k+1)=z_2(k)-\beta_1\varepsilon_1(k)+bu(k) \\ z_2(k+1)=-\beta_2\varepsilon_1(k) \end{cases} \tag{12}$$

where $z_2$ is the expanded state variable, which represents the sum of unmodeled internal dynamics and external disturbances.

According to reference [18], $\beta_1$ and $\beta_2$ of (12), have the following relationship:

$$\begin{cases} \beta_1=2\omega \\ \beta_2=\omega^2 \end{cases} \tag{13}$$

where $\omega$ is new parameter to be calibrated. By substituting (10) and (13) into (12), a new ESO expression can be obtained:

$$\begin{cases} \varepsilon(k)=z_1(k)-y(k) \\ z_1(k+1)=\dfrac{30num_{stk}(z_2(k)-2\omega\varepsilon_1(k)+bu(k))}{n_e(k)num_{cycl}}+z_1(k) \\ z_2(k+1)=-\dfrac{30num_{stk}\omega^2\varepsilon_1(k)}{n_e(k)num_{cycl}}+z_2(k) \end{cases} \tag{14}$$

The linearized form of NEF can be expressed as:

$$\begin{cases} e_1(k)=v_1(k)-z_1(k) \\ u_0(k)=\zeta e_1(k) \end{cases} \tag{15}$$

where $\zeta$ is parameter to be calibrated.

The input of MVEM can be represented as:

$$u(k)=\frac{\zeta(v_1(k)-z_1(k))-z_2(k)}{b} \tag{16}$$

In the controller designed earlier, $r_0$, $h_0$, $\omega$, $\zeta$ and $b$ are five calibrated parameters. Among them, $r_0$ and $h_0$ do not have a coupling relationship with the other three parameters and can be calibrated separately according to requirements. And the calibration process is simple.

Considering the strong nonlinearity of diesel engine speed control, a set of parameters is difficult to achieve optimal control effects under all operating conditions. If all operating conditions are calibrated separately, it will consume a lot of resources, and as the engine wears and ages, the parameters corresponding to the optimal control will also migrate. Therefore, this manuscript chooses the BAS algorithm to perform online real-time optimization on the remaining three parameters of ADRC. When the speed offset is greater than or equal to 5rpm, the parameter adjustment function of BAS is activated. The calculation of the BAS module is also fixed phase, consistent with ADRC, which means that an operation is performed between every two fuel injections. Taking an update to $\omega$ as an example, the execution logic of BAS is shown in Fig. 3.

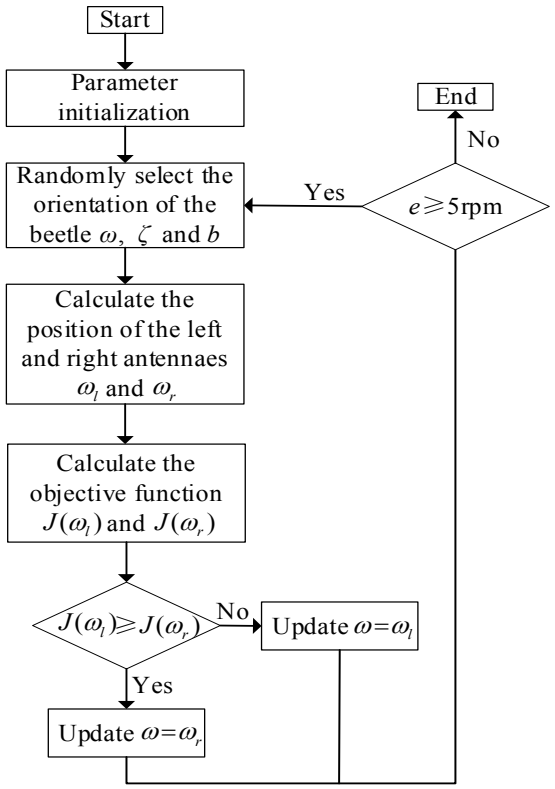


Figure 3. The execution logic of BAS

In ADRC, there is a strong coupling effect between the control parameters. If the optimal control effect is achieved simply by adjusting one of the parameters and fixing the other two to achieve the optimal control effect under the condition, it is probable that it is only a local optimal solution, which will waste computational resources and make the control process converge slowly. As can be seen from Fig. 3, the parameters updated by the BAS designed in this manuscript are randomized during each iteration. And, because it is online optimization, in order to ensure the stability of speed control, this manuscript does not have the maximum iteration step limit, but designed the parameter variation range. The objective function used in BAS is:

$$J(k)=\kappa_1(v_1(k)-n_e(k))^2+\kappa_2(n_e(k)-z_1(k))^2 +(1-\kappa_1-\kappa_2)u(k)^2 \quad (17)$$

where $\kappa_1$ and $\kappa_2$ are calibrated parameters, and $\begin{cases}\kappa_1+\kappa_2<1\\0<\kappa_1<1\\0<\kappa_2<1\end{cases}$.

In this manuscript, the parameters of the ADRC are adjusted online by the BAS, and the adjustment process is of variable step size, whose time step is related to the speed. In order to ensure that the speed of parameter adjustment is not affected by the change of diesel engine speed, this manuscript proposes the following equation, which is used to update the antennae length of the BAS in real time:

$$\delta_{step}=\frac{n_{e,idle}}{n_e}\delta_{step,0} \quad (18)$$

where $n_{e,idle}$ is the speed of the diesel engine at idle and $\delta_{step,0}$ is the initial antenna length of the BAS.

## IV. CONCLUSIONS

Based on the experience of manual calibration of the ADRC, it is found that when the diesel engine speed changes, adjusting the parameter w of the ESO alone still achieves excellent speed control under all diesel engine operating conditions. This is because ESO treats the control error due to the deviation of the other two parameters as a disturbance. Therefore, as long as the disturbance observation speed and accuracy always meet the requirements, it is completely possible to reduce the three parameters to be optimized to one at the expense of a small amount of speed control performance. And such an improvement can reduce the amount of controller computation and increase the efficiency of parameter search. So, this manuscript further designs SP-VABAS-ADRC. Meanwhile, in order to carry out the controller performance validation, this manuscript also designs VP-PID. this controller contains five groups of parameters, which are used to control at different speeds. Linear interpolation is used to update the VP-PID parameters when the speed is not at the calibration point. And then software simulation is carried out to verify the control effect of the controller designed in this manuscript and compare it with the VP-PID controller. The simulation results are shown in Fig. 4 to Fig. 8:

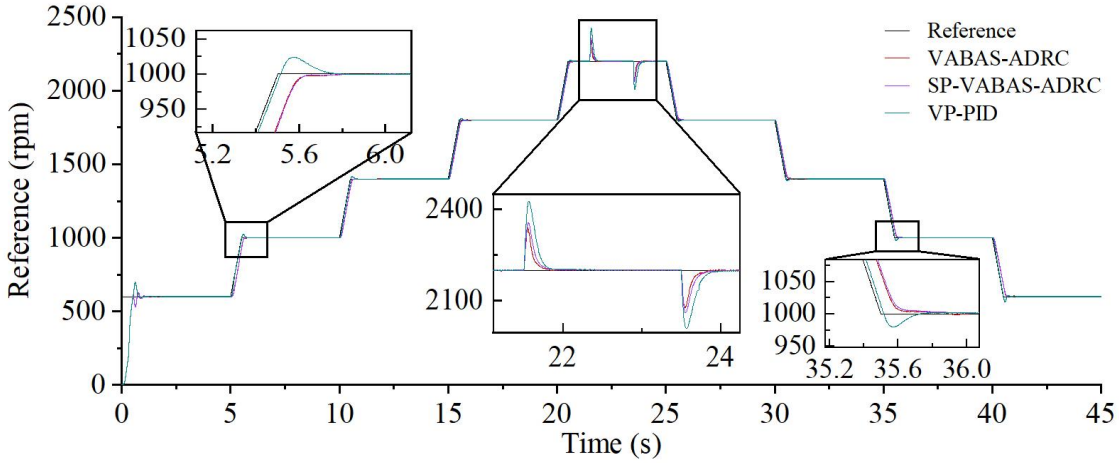


Figure 4. The speed control effect of VABAS-ADRC

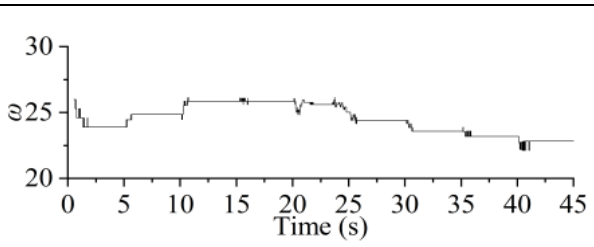


Figure 5. Variation of the ω of VABAS-ADRC

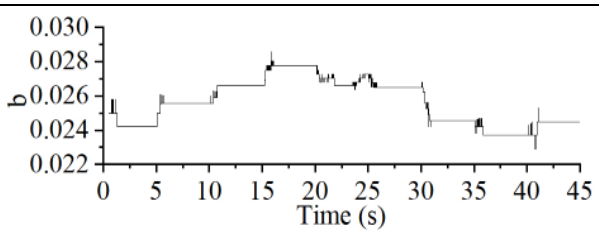


Figure 6. Variation of the b of VABAS-ADRC

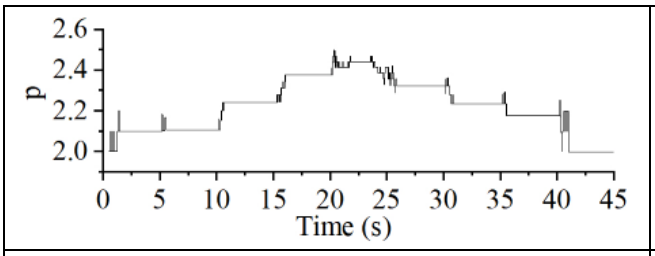


Figure 7. Variation of the p of VABAS-ADRC

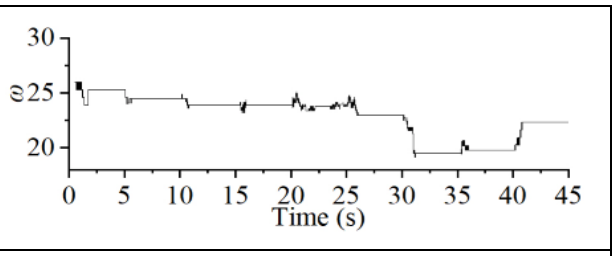


Figure 8. Variation of the ω of SP-VABAS-ADRC

Fig. 4 shows the speed control effect of different controllers during acceleration and deceleration and sudden load change, and Fig. 5 to Fig. 8 show the parameter search process corresponding to Fig. 4. Analyzing the experimental results, it can be seen that a small amount of control overshoot occurs in VA-PID during acceleration and deceleration, but VABAS-ADRC basically achieves the tracking effect without overshoot. When the load is loaded and unloaded suddenly, although the convergence time of speed control of the two controllers is basically the same, it is obvious that the corresponding speed fluctuation of the VABAS-ADRC is smaller. Therefore, the VABAS-ADRC has a better control performance than the VP-PID. Comparing the control effect of VABAS-ADRC and SP-VABAS-ADRC, it is found that the control performance of the two is similar, except that the speed fluctuation of SP-VABAS-ADRC increases slightly when the load changes suddenly, but this is basically within the allowable range.

Combined with the analysis of Fig. 5 to Fig. 8, the controller designed in this manuscript has excellent control performance, and the calculation is small, when the controller parameters are unreasonable, the controller parameters can be optimized in a short period of time, the number of iterative steps is small, and it has the potential to be applied in engineering practice.

## REFERENCES


[1] Wu L G, Liu J X, Vazquez S, et al. "Sliding Mode Control in Power Converters and Drives: A Review," *Ieee-Caa Journal of Automatica Sinica*, vol. 9 pp. 392-406, Mar 2022.

[2] Utkin V. "Variable structure systems with sliding modes," *IEEE Transactions on Automatic Control,* vol. 22 pp. 212-222, 1977.

[3] Senthilkumar R, Balamurugan R. "Adaptive Fuzzy-Based SMC for Controlling Torque Ripples in Brushless DC Motor Drive Applications," *Cybernetics and Systems,* vol. 54 pp. 1132-1153, Oct 3 2023.

[4] Du H B, Chen X P, Wen G H, et al. "Discrete-Time Fast Terminal Sliding Mode Control for Permanent Magnet Linear Motor," *Ieee Transactions on Industrial Electronics,* vol. 65 pp. 9916-9927, Dec 2018.

[5] Wang X R, Sun S H, Van Kampen E J, et al. "Quadrotor Fault Tolerant Incremental Sliding Mode Control driven by Sliding Mode Disturbance Observers," *Aerospace Science and Technology,* vol. 87 pp. 417-430, Apr 2019.

[6] Medina L, Guerra G, Herrera M, et al. "Trajectory tracking for non-holonomic mobile robots: A comparison of sliding mode control approaches," *Results in Engineering,* vol. 22 pp., Jun 2024.

[7] Shi Y, Zhang K W. "Advanced model predictive control framework for autonomous intelligent mechatronic systems: A tutorial overview and perspectives," *Annual Reviews in Control,* vol. 52 pp. 170-196, 2021.

[8] Wang Z Y, Tan W G Y, Rangaiah G P, et al. "Machine learning aided model predictive control with multi-objective optimization and multi-criteria decision making," *Computers & Chemical Engineering,* vol. 179 pp., Nov 2023.

[9] Yu D W, Yu D L. "Modeling a multivariable reactor and on-line model predictive control," *Isa Transactions,* vol. 44 pp. 539-559, Oct 2005.

[10] Shu H Y, Li X M, Liu Y F, et al. "Model Predictive Control With Disturbance Observer for Marine Diesel Engine Speed Control," *Ieee Access,* vol. 11 pp. 49300-49318, 2023.

[11] Zenere A, Zorzi M. "On the coupling of model predictive control and robust Kalman filtering," *Iet Control Theory and Applications,* vol. 12 pp. 1873-1881, Sep 4 2018.

[12] Wu C, Song K, Xie H. "Control of the common rail pressure in gasoline engines through an extended state observer based MPC," *Control Theory and Technology,* vol. 17 pp. 156-166, May 2019.

[13] Gao Z. "Active disturbance rejection control: From an enduring idea to an emerging technology," in *10th International Workshop on Robot Motion and Control, RoMoCo 2015*, Poznan, Poland, 2015, pp. 269-282.

[14] Han J Q, "Auto-disturbances-rejection Controller and Its Applications," Belmont, *Control and Decision,* 1998.

[15] Wang Y Q, Zhang G C, Shi Z B, et al. "Finite-Time Speed Control of Marine Diesel Engine Based on ADRC," *Mathematical Problems in Engineering,* vol. 2020 pp., Feb 22 2020.

[16] Wang R, Li X, Zhang J, et al. "Speed Control for a Marine Diesel Engine Based on the Combined Linear-Nonlinear Active Disturbance Rejection Control," *Mathematical Problems in Engineering,* vol. 2018, 2018.

[17] Liu Z, Chen T, Zhou P, et al. "Modeling and Control Strategy Research on Diesel Engine HighPressure Common Rail System," in *43rd Chinese Control Conference, CCC 2024, July 28,* Kunming, China, 2024, pp. 260-267.

[18] Han J Q, *Active Disturbance Rejection Control Technology: Control technology for Estimating compensating Uncertainties*. Beijing, National Defense Industry Press, 2008, pp. 210-210.